Journal of Food Engineering 239 (2018) 15–25

Contents lists available at ScienceDirect

Journal of Food Engineering

journal homepage: www.elsevier.com/locate/jfoodeng

Cherry (*Prunus avium*) phenolic compounds for antioxidant preservation at food interfaces

Maria F. Basanta[a,e], Ana M. Rojas[a,e], Manuela R. Martinefski[b,d], Valeria P. Tripodi[c,e], Maria D. De'Nobili[a,e], Eliana N. Fissore[a,e,*]

[a] Departamento de Industrias, Facultad de Ciencias Exactas y Naturales, University of Buenos Aires, Ciudad Universitaria, C1428BGA, Buenos Aires, Argentina
[b] Departamento de Química Analítica y Fisicoquímica, Facultad de Farmacia y Bioquímica, University of Buenos Aires, Junin 954, C1113AAD, Buenos Aires, Argentina
[c] Departamento de Tecnología Farmacéutica, Facultad de Farmacia y Bioquímica, University of Buenos Aires, Junin 954, C1113AAD, Buenos Aires, Argentina
[d] Fellow of CONICET, Argentina
[e] Member of CONICET, Argentina

ARTICLE INFO

Keywords:
Cherry anthocyanins
Flavonols
Hydroxycinnamic acids
Quercetin-3-*O*-Rutinoside
Antioxidant pectin film
Total phenolics-release

ABSTRACT

Cherry phenolics extracted by 90°C-water were loaded in a low-methoxyl-pectin (LMP) film for antioxidant preservation. Dark red films (pH = 3.46) contained flavonols (dihydrokaempferol-glucoside, quercetin-3-*O*-rutinoside), hydroxycinnamic acids (neochlorogenic, chlorogenic, 3-*p*-coumaroylquinic acids), and anthocyanins (cyanidin-3-O-glucoside, cyanidin-3-O-rutinoside), with a 6.97×10^{-12} m^2/s diffusion coefficient. Phenolics' stability was studied at constant relative humidity (RH: 57.7; 75.2%) and 25.0 °C. The pseudo-first-order degradation rate was the highest ($t_{1/2}$ = 3-2 months) and increased with the equilibration RH in darkness for anthocyanins, with simultaneous red vanishing by water nucleophilic attack. Instead, flavonols remained stable ($t_{1/2}$ > 1.5 years). Light (75.2%RH) induced the highest phenolics-degradation-rates, especially for anthocyanins ($t_{1/2}$ = 11d), sensitizer, and film red color. Flavonols-decay was the slowest ($t_{1/2}$ = 7–12 months). Antioxidant capacity paralleled phenolics-content. Hydroxycinnamic acids followed by flavonols could scavenge the singlet oxygen. Light-triggered LMP-matrix—phenolic interactions were determined, producing the lowest film water content and deformability. Cherry phenolics stabilized as a colored film constituted a food preserving antioxidant barrier.

1. Introduction

Phenolic compounds are secondary plant metabolites that have one phenol ring (phenolic acids, phenolic alcohols) or several aromatic rings with one or more hydroxyl groups (polyphenols) (Borges et al., 2017). In vivo and in vitro experiments have revealed that most phenolics, especially polyphenols, have many different bioactivities such as antioxidation, digestive enzyme inhibition, and anti-inflammation (Huang et al., 2017). Antioxidants play a vital role in free radical scavenging and chain breaking of oxidation reactions both in vivo and in vitro. The potential uses of antioxidants include the prevention of diseases related to oxidative stress in humans and also of oxidative reactions in food, pharmaceuticals, and cosmetic products (Qadir et al., 2017).

Utilization of synthetic antioxidants such as propyl gallate, butylated hydroxyanisole (BHA), and butylated hydroxytoluene (BHT) in foods leads to many side effects, and the use of synthetic antioxidants is constantly under revision by the FDA (Taghvaei and Jafari, 2015). Consequently, an increased interest exists in finding natural antioxidant substances capable of scavenging free radicals and hindering oxidative rancidity, retarding food spoilage (Qadir et al., 2017). The application of phenolic compounds as functional ingredients is widely studied. In a complex food system, interactions between these bioactive compounds and the food matrix may affect the quality of polyphenol-rich food products, as these interactions impact both the bioavailability and bioactivity of the phenolic compounds (Gómez-Mascaraque et al., 2017). Compartmentalization of phenolics into an edible film can overcome negative interactions between these compounds and other food preservatives and food components used in a food system, while it can also increase phenolics-stability. Moreover, a localized activity of phenolics loaded in films can be the way to achieve higher efficiency as antioxidants, and to enhance availability. Additionally, some phenolic compounds can color the edible films, which could make them attractive for special purposes.

Abbreviations: LMP, low-methoxyl-pectin; DPPH, 2,2-diphenyl-1-picrylhydrazyl free radical assay; FRAP, ferric reducing ability power assay; RH, relative humidity; $t_{1/2}$, half-life time

* Corresponding author. Departamento de Industrias, Facultad de Ciencias Exactas y Naturales, University of Buenos Aires, Ciudad Universitaria, C1428BGA, Buenos Aires, Argentina.
E-mail addresses: eliana@di.fcen.uba.ar, elianafissore@gmail.com (E.N. Fissore).

https://doi.org/10.1016/j.jfoodeng.2018.06.028
Received 15 January 2018; Received in revised form 14 June 2018; Accepted 26 June 2018
Available online 26 June 2018
0260-8774/

Thermal blanching is an essential operation for fruit and vegetable processing developed for inactivation of enzymes, which also enhances drying rate and product quality. It is an energy intensive process, and generates wastewater. The latter contains soluble solids and chemical oxygen demand due to leaching and dissolution of sugars, proteins, carbohydrates and water-soluble minerals (Xiao et al., 2017), as well as of polyphenols (Chaovanalikit and Wrolstad, 2004). When not well treated before discharge, this wastewater can cause environmental pollution such as eutrophication (Xiao et al., 2017). Between November and December cherry is harvested in Argentina, Chile, Australia and New Zealand (Cittadini, 2007). Smaller, misshapen, bruised and/or overripe cherries can be upgraded for extraction of antioxidants and dietary fiber. In this process, cherry tissue homogenate should be blanched for stabilization.

Cherry phenolics extracted by 90°C-water from a sugar-exhausted homogenate were applied to the development of a LMP film for antioxidant preservation at food interfaces, by phenolics-stabilization in the polymeric network. In this context, the antioxidant activity, phenolic composition, release behavior and mechanical properties of films were analyzed, as well as the phenolic and color stabilities by film storage at 57.7 or 75.2% RH in the dark or at 75.2% RH in the light, at 25.0 °C, in order to determine the influence of deleterious factors on the half-life time as active film.

2. Materials and methods

2.1. Chemicals

Deionized water was used (MilliQ, Millipore, USA). Food grade pectin with a low degree of methyl esterification (GENU pectin type LM-12 CG) was a gift from CP Kelco (Denmark). Chemical characteristics of this pectin product were determined by De'Nobili et al. (2013a). Sucrose (34.3% w/w) is added by the manufacturer for standardization. Potassium sorbate, DPPH (2,2-diphenyl-1-picrylhydrazyl), TPTZ (2,4,6-tripyridyl-100 s-triazine), $FeCl_3{\cdot}6H_2O$, chlorogenic acid (5-O-caffeoylquinic acid), quercetin-3-O-rutinoside, and cyanidin-3-O-glucoside were from Sigma-Aldrich (Saint Louis, USA), while the other chemicals were from Merck (Argentina's branch).

2.2. Cherry aqueous extract enriched in polyphenols

Cherries harvested in Rio Negro province (Argentina) were carefully washed with detergent and rinsed with tap and deionized water. Stones were removed and water (20 °C) was added (500 g fruit:300 mL water), the mixture was then homogenized (Sorvall Omni Mixer, USA) for 1 min, and finally filtered through a nylon net. The filtrate was discarded and the retentate was recovered and submitted to a second washing to eliminate sugars, and then filtered. The final retentate was poured into 1500 mL of deionized water at 90 °C constant for 2 min while stirring (600 rpm) for blanching. The residue recovered after vacuum filtration through a glass fiber filter (Whatman GF/C, UK) was rapidly cooled, being applied to the dietary fiber extraction for a future research work, while the filtrated aqueous solution was recovered for the following edible film development.

2.3. Film making procedure

300.00 g of total film making solution was elaborated per batch. It was made into a 1 L-glass beaker containing 295.00 g of the aqueous extract obtained in section 2.2, where 8.00 g of the commercial GENU TM pectin containing 5.25 g of LMP were dispersed under controlled and constant high-speed shear. Glycerol (5.0000 g) for plasticization, potassium sorbate (0.0900 g) for antimicrobial preservation, and $CaCl_2.2\ H_2O$ (0.5000 g) were added with the system at 85 °C, as explained by De'Nobili et al. (2016). The total weight of the solution was finally completed to 300.00 g with water. Three batches of this solution were prepared.

By casting (2.5 h, 60 °C under air convection) of the corresponding batch of the film making solution distributed in *a constant weight* among identified polyestyrene plates (55 mm-diameter), three film batches (triplicate of assay) were produced (De'Nobili et al., 2016). In order to maintain a constant RH for film equilibration or equilibrium relative humidity (ERH), the identified films obtained in the three batches were distributed among desiccators (Nalgene, USA) containing a saturated (standard) solution of known water activity ($a_W{}^o$), either NaBr ($a_W{}^o = 0.577$) or NaCl ($a_W{}^o = 0.752$):

$$a_W^o = \frac{RH\%}{100} = \frac{ERH}{100} \quad (1)$$

Storage was then performed at constant 57.7 or 75.2%RH (eq. (1)) and 25.0 °C in light-protected desiccators, or at 75.2%RH in a third desiccator placed at 20 cm from the light source (white led device, cold light, 1550 lumens, 20 W). A thermometer was placed into this desiccator to check the real temperature. Film equilibration was followed by the daily measurement of the a_W in film samples (Decagon AquaLab, Series 3 Water activity meter, USA), according to De'Nobili et al. (2016). After films attained the equilibrium $a_W{}^o$ (eq. (1)), thickness was measured at three different locations in each of ten films with a digital micrometer (Mitutoyo, Kawasaki, Japan).

2.4. Chemical analysis

2.4.1. Determination of polysaccharides

Total carbohydrates' and uronic acid contents were determined in the cherry aqueous extract (section 2.2) according to Basanta et al. (2016).

2.4.2. Extraction of phenolic compounds for quantification

Phenolics were extracted twice from the cherry aqueous extract obtained as explained in section 2.2 or from each cut film by sonication for 22 min with 5 mL acetone/water/acetic acid (70:29.5:0.5 v/v/v) solution, followed by centrifugation (10 min), supernatants' separation, and reduced pressure evaporation at 35.0 °C (Basanta et al., 2016). The aqueous residue was filtered through an activated Sep-Pack C-18 solid phase extraction cartridge (Waters, Milford, MA, USA), then washed with water, and the retained phenolics were eluted with 1.000 mL of methanol, and filtered through a 0.45 μm nylon.

2.4.3. Analysis of phenolic compounds

The filtered methanolic extract was injected manually (volume: 20 μL) into a Waters 1525 HPLC (Milford, MA, USA) equipped with a binary pump and photodiode array detector. A Luna C18 column (250 × 4.0 mm, 5 μm particle size; Phenomenex, USA) was used. The mobile phase was composed of water (1% formic acid) (A) and methanol (B), using a 0.8 mL/min flow rate. A linear gradient was used starting with 10% of B up to reach 60% at 50 min. Spectral data from all peaks were accumulated in the 200–400 nm range. The HPLC-MS/MS analyses were performed on an Ultimate 3000 system (Thermo Fisher Scientific Inc, USA) coupled to a TSQ Quantum Access Max triple quadrupole mass spectrometer (Thermo Fisher Scientific Inc, USA), equipped with an electrospray ionization (ESI) source, and operated in multiple reaction monitoring (MRM) in the negative ion mode. The optimal values for MS parameters were 3500 V for spray voltage, 30 and 45 for sheath and auxiliary gas pressure, respectively, 300 °C for capillary temperature. The mass spectrometer was employed in MS/MS mode using argon as collision gas. The HPLC was equipped with an autosampler, and a quaternary pump. The same chromatographic conditions described above were used.

Quantification of the identified analytes was performed by HPLC-DAD using the external standard method. Hydroxycinnamic acids were quantified as chlorogenic acid (5-*O*-caffeoylquinic acid) at 320 nm, flavonols as quercetin-3-*O*-rutinoside at 360 nm, and anthocyanins as

Table 1
Composition[a] of the water obtained after blanching of cherry homogenate, used for the edible film development.

	Phenolic compounds	mg/100 mL of cherry water	Retention time (min)	HPLC-UV-DAD (nm)	HPLC-ESIMS (m/z)
Hydroxycinnamic acids	neochlorogenic acid	2.3 ± 0.6	12.3	324	353/191
	3-*p*-coumaroylquinic acid	0.65 ± 0.09	16	310	337/191
	chlorogenic acid	0.56 ± 0.06	18	324	353/191
Anthocyanins	cyanidin-3-O-glucoside	4.3 ± 0.5	23	519	593/284
	cyanidin-3-O-rutinoside		23	519	447/284
Flavonols	dihydrokaempferol-glucoside	0.78 ± 0.03	29	343	447/284
	quercetin-3-O-rutinoside	0.95 ± 0.30	36	354	609/301
Total phenolics		9.5 ± 0.6			

[a] Mean and standard deviation ($n = 3$) are reported.

cyanidin-3-*O*-glucoside at 520 nm.

The content of each phenolic compound in the cherry aqueous extract or wastewater of blanching was expressed as mg/100 mL (Table 1).

The content of a given phenolic compound [$weight_{Ph}(t)$] was determined as explained in each of the three films, each taken from a batch at a given time of storage (t) (eq. (2)), including at $t = 0$ (eq. (3)). Since the weight of the film making solution and, hence, of the phenolic compounds initially dispensed in each identified plate before casting was known ["$weight_{Ph,\ film}$ (o,*loaded*)"], the relative proportion of the phenolics contained in the film at a storage time [$C_{Ph}(t)$] (eq. (2)), including at $t = 0$ (eq. (3)), was calculated as follows:

$$C_{Ph}(t) = \frac{weight_{Ph}(t)}{weight_{Ph,film}(o,\ loaded)} \tag{2}$$

$$\Rightarrow \quad C_{Ph}(t=0) = C_{Ph_O} = \frac{weight_{Ph}(o)}{weight_{Ph,film}(o,\ loaded)} \approx 1.00 \tag{3}$$

2.5. Antioxidant capacity

Aliquots of the 1.000-mL-methanolic extract obtained from each film (2.4.2. Section) were evaluated in their radical scavenging activity through the DPPH assay, and ferric reducing antioxidant power by FRAP test, according to Idrovo Encalada et al. (2016). L-(+)-ascorbic acid dissolved in methanol was used as standard.

2.6. Film characterization

The following assays (2.6.1.-2.6.6.) were performed in the films after their equilibration (eq. (1)) at 57.7 or 75.2% RH. Tests were made at least in triplicate, taking a film from each of the three batches produced (see section 2.3).

2.6.1. Measurement of pH

The pH was determined on the film-forming solutions as well as on the films equilibrated at the corresponding RH using a bulb-combined glass electrode (Mettler Inlab Viscous Pro, Germany) or a flat surface electrode (Phoenix, AZ, USA) connected to a pH meter (Mettler S220 Kit, Germany). Film pH was determined after a slight surface hydration with 20.0 µL of deionized water (De'Nobili et al., 2013b). Standard buffer solutions (pH 4.00 and 7.02) were used for calibration.

2.6.2. Color

Measurement of L^*, a^*, and b^* (CIE-Lab) color parameters was performed on films and cherry aqueous extract with a Minolta colorimeter (Minolta CM-600D, Tokyo, Japan), using D-65 sodium illuminant and a 2° observer, according to Idrovo Encalada et al. (2016).

2.6.3. Water content

Equilibrated films were sampled, cut into pieces smaller than 1-mm size, weighed (0.0001 g precision) and placed into small light glass containers. Dehydration was performed in a vacuum oven at 70 °C to avoid chemical decomposition, until a constant weight was reached, which involved approximately 24 days for the LMP films developed. Determinations were performed on six film specimens. Moisture or water content was calculated on dry basis.

2.6.4. Differential scanning calorimetry (DSC)

Films equilibrated by storage in the dark either at 0% (anhydrous $CaCl_2$ desiccator), 57.7% or 75.2% RH, or in the light at 75.2% RH were studied through DSC. A modulated differential scanning calorimeter (MDSC, TA Instruments, USA) was used to determine the calorimetric profile, including the glass transition temperature (T_g) at the midpoint, from the second scan of the heat flow versus temperature performed on an equilibrated film sample (10–15 mg) placed into an hermetically sealed 40-µL aluminum medium pressure pan. An empty pan served as reference. Temperature was brought down to −140 °C (20 °C/min) followed by a 5-min isotherm. A heating ramp was then performed up to 40 °C (10 °C/min), followed by a second decrease in temperature to −140 °C (20 °C/min), and a 5-min isotherm. Afterwards, a second heating ramp was performed up to 100 °C (10 °C/min), from which possible first order transitions and T_g values were analyzed. A ± 0.5 °C every 40 s modulation was applied. The first derivative of the heat flow was calculated to clearly determine the T_g values from each minimum. MDSC was periodically calibrated with a sapphire disk, in the full temperature range at which the equipment is usually employed.

2.6.5. Tensile assays

The uniaxial tensile test was performed until rupture (5 mm/min-constant crosshead speed) on equilibrated film sample strips (25.0 mm × 6.0 mm) cut with parallel sides, using an Instron Testing Machine (model 3345, USA). The normal stress (σ_{break}) and strain or relative deformation (ε_{break}) at film rupture were calculated as:

$$\sigma_{break} = F_{break}/A_O \tag{4}$$

$$\varepsilon_{break} = (L_{break} - L_O)/L_O \tag{5}$$

where A_O is the initial cross sectional area of the film sample; L_O is the initial gap between clamps (20 mm) that maintained the strip fixed with a 0.1 N pre-load; F_{break} and L_{break} are the force and length respectively reached at film rupture. The tensile strength (TS) was then calculated as:

$$TS_{break} = \sigma_{break}/\varepsilon_{break} \tag{6}$$

Only for the tensile evaluation, films were also made as explained in section 2.3 but without the addition of cherry extract, which were called "blank" films.

2.6.6. Fast Fourier transformed infrared spectroscopy (FT-IR)

Spectra were recorded on a Nicolet 8700 (Thermo Scientific Nicolet, USA) spectrometer equipped with a diamond attenuated total reflection (ATR) device for films, as explained by Pérez et al. (2009). Lyophilized cherry aqueous extract loaded in a KBr pellet was measured by transmission.

2.7. Release of total phenolic compounds by films

The release experiment was performed with film samples at 25.0 °C according to Flores et al. (2007), but using deionized water (pH 7.00) as release medium. The amount of total phenolics released per g of film was determined as explained in 2.4.2 and 2.4.3 sections. Calculation of the diffusion coefficient (D) of total phenolics was performed through a model that considered both the mass transport related to the Brownian motions (Fick's second law) and the polymer relaxation mechanisms (Flores et al., 2007). The deviation of the transport mechanism from the ideal Fickian behavior (X_F) and the characteristic relaxation time associated to the polymer (τ) were also determined. As X_F is defined as the ratio between the amount of low molecular weight compound (total phenolics) released at equilibrium as a consequence of the stochastic phenomena (M_F^{eq}), and the amount of the low molecular weight compound released at equilibrium (M^{eq}), where:

$$M^{eq} = M_F^{eq} + M_R^{eq} \tag{7}$$

the equation (8) can be finally obtained (Flores et al., 2007):

$$M(t) = M^{eq}\cdot\left\{X_F\cdot\left\{1 - \frac{8}{\pi^2}\cdot\sum_{n=0}^{n=\infty}\frac{1}{(2\cdot n+1)^2}\cdot\exp\left\{-D\cdot(2\cdot n+1)^2\cdot\pi^2\cdot\frac{t}{\ell^2}\right\}\right\} + (1 - X_F)\cdot\left[1 - \exp\left(-\frac{t}{\tau}\right)\right]\right\} \tag{8}$$

which permitted us to calculate, by using a Matlab program for fitting to experimental data, the total amount of the phenolics released at time t, [$M(t)$], and the diffusion coefficient (D) by considering both (a) the contribution of the stochastic phenomena to the amount of the phenolics released at time t, $M_F(t)$, according to the diffusion through a plane sheet of ℓ thickness, with constant boundary conditions, for which the Fick's second law is solved, and (b) the polymer relaxation driven by the distance of the system from the equilibrium. M_R^{eq} in the equation (7) is the amount of low molecular weight compound (total phenolics) released at equilibrium as a consequence of the polymer relaxation.

By definition, X_F ranges from 0 to 1. When X_F is equal to 1, equation (8) is the solution of the Fick's second law, but when X_F is equal to 0, an anomalous diffusion is obtained.

2.8. Statistical analyses

The results are reported as the average and standard deviation (SD) for n replicates. Analysis of covariance (ANCOVA) was applied for comparison of slopes (k_{Ph}') in linear regressions, as indicated by Sokal and Rohlf (2000). Statistical analyses of results were performed through ANOVA (α: 0.05), followed by Tukey's significance difference test. Spearman's correlation was applied as a measure of the strength of the association between variables such as each color parameter (a^*, b^* or L^*) and the $C_{Ph}(t)$, at each storage time (Hauke and Kossowski, 2011). The GraphPad Prism software (version 5.00, 2007, USA) was used.

3. Results and discussion

3.1. Cherry aqueous extract used for film making and characteristics of the casted films

The aqueous extract used for the edible film development was that obtained after blanching at 90 °C of the cherry homogenate, previously washed to eliminate simple sugars. As a consequence, very low content of total carbohydrates (1.4 ± 0.4% w/v) and a non detectable level of uronic acids (pectins) were determined. Water extractable phenolics' composition is reported in Table 1. They were identified as neochlorogenic, chlorogenic and 3-*p*-coumaroylquinic acids (hydroxycynnamic acids), cyanidin-3-*O*-glucoside and cyanidin-3-*O*-rutinoside (anthocyanins), and dihydrokaempferol-glucoside and quercetin-3-*O*-rutinoside (flavonols). The highest contents corresponded to the anthocyanins, responsible for the red color, and neochlorogenic acid. Color parameters of the transparent cherry aqueous extract of pH 4.26 were 10.9 ± 0.9% for L^*, 15.9 ± 0.7 for a^* and 6.6 ± 0.4 for b^*. The low lightness (L^*) value indicated a dark color.

The film forming solution containing LMP as the polymer, glycerol, potassium sorbate (pK_a sorbic acid = 4.76; 25 °C) and the phenolics had a pH of 2.30 ± 0.04.

The LMP-films obtained after casting were homogeneous and flexible, being plasticized by glycerol [48.75 g/100 g (pectin + glycerol)]. Films were transparent and dark (L^* = 32 ± 1%) red (a^* = +49.7 ± 0.6; b^* = +15.5 ± 0.3) at their pH of 3.46 ± 0.04. The film composition in phenolics is that summarized in Table 2 through the respective retention times of phenolics, showing that it coincided with the composition reported in Table 1 for the cherry aqueous extract loaded. The initial concentration of total phenolics on film samples, calculated as the sum of each determined phenolic compound, was 13.6 mg/100 g dried film (Table 2). This value meant that the retention of phenolics reached after drying was ≈99.4%, as calculated through the eq. (3). Anthocyanins may exist in at least four

Table 2
Initial composition[a] in phenolics of the casted films, and parameters obtained from the release assay of total phenolic compounds from films.

Retention time (min)						**Total phenolics' content**
12.3	**16**	**18**	**23**	**29**	**36**	
mg phenolic compound/100 g dry mass of film						
3.7 ± 0.4	1.12 ± 0.06	1.00 ± 0.06	5.1 ± 0.6	1.17 ± 0.07	1.5 ± 0.2	13.6 ± 0.6

Release of total phenolic compounds					
D (m^2/s)	X_F	T (s^{-1})	M^{eq} (mg/g film)	$M^{eq}/M_{(t=0)}$	$\bar{e}$%
6.97×10^{-12}	0.9016	1587.6	0.740	0.882	−3.885

[a]Mean and standard deviation (n = 3) are reported.
D, diffusion coefficient of total phenolics. X_F, deviation of the transport mechanism from the ideal Fickian behavior.
τ, relaxation time associated to polymer relaxation. M^{eq}, g of total phenolics at time t per g of film. $M_{(t=0)}$, g of total phenolics initially loaded per g of film. $\bar{e}$%, percentage of mean error.

Table 3
Properties of the equilibrated LMP-films loaded with cherry phenolics.

RH	Water content[a] (g/100 g dm)	Thickness[a] (mm)	T_g (C)	Change in specific heat at the glass transition [J/g (dm) K]
57.7% (dark)	18.9 ± 0.7[a]	0.157 ± 0.006[a]	−90.93	1.665
			−75.72	2.199
			−6.36	3.083
			5.61	3.143
75.2% (dark)	20.0 ± 0.7[a]	0.152 ± 0.004[a]	−91.78	1.431
			−1.74	2.651
			10.61	2.722
75.2% (Light)	12.0 ± 0.9[b]	0.141 ± 0.012[b]	−92.09	1.226
			−73.60	1.711
			−9.75	2.420
0% (dark)			−92.45	1.226
			−46.60	1.809
			−8.99	2.309

[a]Mean and standard deviation (n = 3) are reported.
The same lower case letter in a column means non-significant differences ($p < 0.05$).
dm: dry mass.

different pH-dependent structural isoforms among which the flavylium cation (red color) arising at pH 1–3 can be the isoform prevalent in the developed films of pH 3.46. Coutinho et al. (2015) determined a pK_a of 3.8 for cyanidin-3-*O*-glucoside in water, which increased to 4.8 in water-depleted media (water concentrations below 0.75 M), thus shifting the equilibrium towards the red-colored form (AH^+) at low water contents. According to the moisture contents determined in films (Table 3), and using as an approximation the equation determined by Coutinho et al. (2015), a pK_a value of 5.50–5.52 for the cyanidin-3-*O*-glucoside loaded in the LMP films can be calculated.

3.2. Release of phenolic compounds from films

The release kinetic of total phenolics from the LMP-films to water was determined at 25.0 °C under convection. The model reported by Flores et al. (2007) fitted satisfactorily (continuous line) the experimental data obtained (Fig. 1). The results reported in Table 2 indicate that the polymer matrix relaxation was superimposed to pure Brownian motion of the mass transfer phenomenon by Fickian mechanism, due to the swelling of the hydrophilic LMP-film matrix, as suggested by the X_F value (< 1) obtained, and relaxation time associated to the polymer (τ) for the diffusion of total phenolics in the amorphous matrix. De'Nobili et al. (2015) demonstrated that the LMP-film loaded with L-(+)-ascorbic acid swelled when placed on a 2% agar-gel, and the degree of swelling determined the average network mesh size and, hence, the water mobility and ascorbic acid diffusion. The $M^{eq,Ph}/M_{(t=0)}$ ratio obtained (Table 2) indicated that once the equilibrium was reached after 40 min of release, a 12% of the initial total phenolic concentration remained entrapped in the LMP matrix.

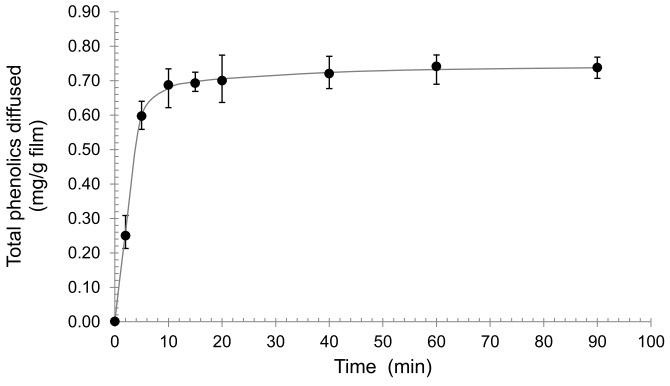

Fig. 1. Profile of cherry phenolics-release from the LMP-film. Experimental points with the standard deviation bar (n = 3), and the continuous line of the model fitted are shown.

By using an analytic solution to the Fick's law applied to the transient state, Benbettaïeb et al. (2016) reported diffusion coefficients of the same order of magnitude than that herein obtained (Table 2), being of 1.69×10^{-12} and 1.48×10^{-12} m^2/s for the release in water at 25 °C, of the ferulic acid respectively loaded in non-irradiated and 60-kGy irradiated chitosan-gelatin edible films. In this case, a 27% of ferulic acid remained entrapped once the equilibrium was reached.

3.3. Moisture content, film thickness and T_g

As determined from the measurement of the film a_W every day, the films stored at constant temperature (25.0 °C) and RH (57.7 or 75.2%) reached the equilibrium (eq. (1)) in the first week of storage. Equilibrated films had a water content of ≈20% w/w on dry mass (Table 3). When stored under light at the measured temperature of 25.0 °C, the film moisture was the lowest determined, allowing inferring that a network change probably occurred, with a consequent reduction in the film capacity to adsorb water at 75.2% RH (eq. (1)). The film thickness did not vary with the RH of film equilibration in the dark, but decreased slightly under light (Table 3), which can be associated to the lower water adsorption capacity of the light-stored film network. As shown as an example in Fig. 2 for the 75.2%-RH equilibrated film that was stored under light, the DSC scans of films did not show any endothermic peak associated to water fusion at ≈0 °C and, hence, the water was strongly adsorbed by the LMP-network, being non-freezable water (De'Nobili et al., 2013b).

More than one T_g value was found for the films equilibrated at the three storage conditions, as pointed by the arrows in the thermogram of Fig. 2. These T_g values were evidenced by the sharp minima in the first derivative of the heat flow. T_g values, and the change in specific heat (Δc_P) that accompanied each glass transition are reported in Table 3. All T_g values were below 25.0 °C and, hence, films were at the amorphous rubbery state during storage. The lowest T_g value was determined at ≈ −90 °C, which can correspond to the plasticization of the polymeric network by glycerol. The lowest Δc_P was associated to this transition (Table 3). By performing the same DSC scans, a similar and unique T_g value was respectively found by De'Nobili et al. (2013a) for LMP films loaded with L-(+)-ascorbic acid, and equilibrated at 57.7% or 75.2% RH. Alginate films loaded with L-(+)-ascorbic and citric acids, stored at 57.7 or 75.2% RH, showed T_g values (−67.39 and −70.02 °C) shifted respectively to lower temperatures (−76.19 and −89.31 °C) as the glycerol plasticizer proportion increased in films, at a given RH of equilibration (De'Nobili et al., 2016). In the present work, a film loaded with phenolics and plasticized by glycerol was also equilibrated at 0% RH to discriminate the water effect on the film network. A T_g value at −92.45 °C was also found in this system (Table 3).

A second T_g value at −75.72 or −73.60 °C was determined for phenolics-films equilibrated at 57.7%RH in the dark and 75.2%RH in the light, respectively, but at −1.74 °C in the 75.2%RH films stored in the dark. In the 0%RH-films, the second T_g value appeared at −46.60 °C (Table 3).

A third T_g value was determined at −6.36 and −9.75 °C for 57.7% equilibrated films in the dark and 75.2%RH in the light, respectively, and at −8.99 °C for the film equilibrated at 0%RH (Table 3). Hence, these T_g values did not seem to be properly related to water plasticization.

A fourth T_g value above 0 °C was only observed for films stored at 57.7% or 75.2% RH in the dark, being of 5.61 °C and 10.61 °C, respectively (Table 3).

Ordered regions corresponded to calcium-crosslinks between LMP chains. More than one value of T_g may indicate heterogeneous

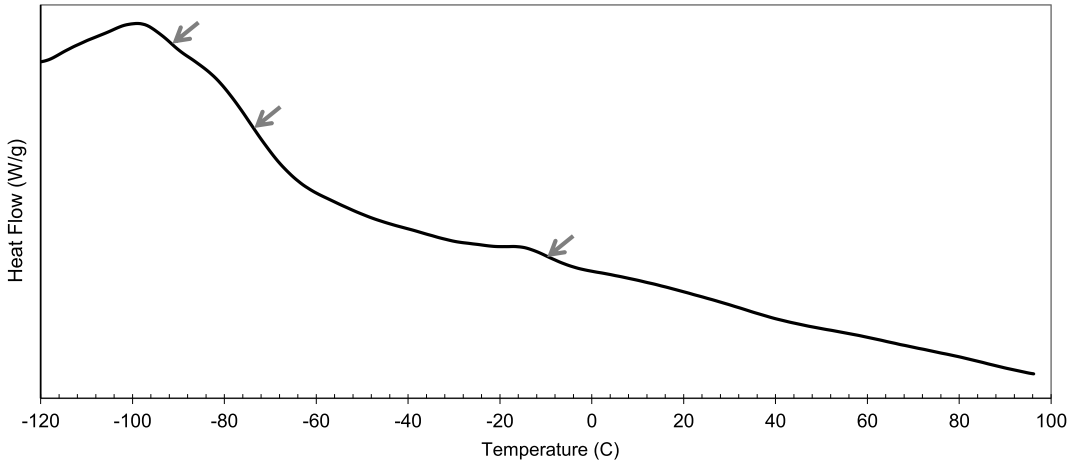

Fig. 2. Thermogram obtained from the heating ramp performed at 10 °C/min in a modulated DSC for the light-75.2%-RH equilibrated LMP-film containing cherry phenolics. Grey arrows indicate the T_g (middle point) localized from the respective minimum of the first derivative.

amorphous regions in films, including less and more restricted, which behaved differently (Liu et al., 2006). Heterogeneity may result from different interactions between (1) the LMP macromolecules that constituted the films and (2) the glycerol, the water adsorbed, and each phenolic compound loaded.

3.4. FT-IR analysis of films

The FT-IR spectra of equilibrated films obtained through the ATR device are shown in Fig. 3, together with the spectrum of the aqueous extract of phenolics. The typical bands corresponding to pectin can be observed in films containing phenolics and equilibrated at 57.7%RH, like the band at 1747 cm^{-1} attributed to the C=O stretching of the esterified carboxyl group. It occurred as a single smaller band than that observed at 1650–1654 cm^{-1}, corresponding to the C=O stretching of the non-esterified carboxylic group. Both bands are then coherent with a low methoxylated pectin. A LMP pectin film made without phenolics and equilibrated at 0%RH produced the same bands (Fig. 3), but films loaded with phenolics and equilibrated at 75.2%RH in the dark gave a more intense band at 1650 cm^{-1}, attributable to the overlapping of the water adsorbed band (Pérez et al., 2009), while simultaneously lost the single band at 1747 cm^{-1} (Fig. 3). The latter can be related to the deep decrease in the number of methyl-ester groups (Fasoli et al., 2016). Studying the chemical conjugation of natural polyphenols (catechin, rutin, quercetin and hesperidin) onto pectin, Ahn et al. (2017) determined that the 1745 cm^{-1} band of the ester C=O stretching vibration recorded from the pure pectin, disappeared in the FT-IR spectra of the conjugated products, while the intensity of the band recorded at ≈1630 cm^{-1} (aromatic C=C- ring) (Vankar and Shuklar, 2011) notably increased. At 75.2%RH, the water mobility in films is sufficiently high and can facilitate the probable interaction between pectin and the cherry phenolic compounds.

The shorter band at 2946 cm^{-1} that corresponds mainly to the OH-stretching in the carboxylic group of pectin, and the band at 2896 cm^{-1} of the C−H (saturated) stretching, characteristic of glycerol plasticizing the LMP-film network, are observed in the spectra of dark stored films (Fig. 3). Also, the OH-stretch broad typical band at ≈ 3291 cm^{-1}, which is reported as characteristic of cell wall polysaccharides (Pérez et al., 2009). The latter band was broadened by the hydrogen bonding of glycerol plasticization (Pérez et al., 2009). All of these bands were deeply modified when films were stored under light (Fig. 3). The OH-stretch produced a sharpened broad band shifted to higher wavenumbers (3459 cm^{-1}), which can probably indicate a noticeably loss of hydrogen-bonding with glycerol (Pérez et al., 2009), while the 2946 and 2896 cm^{-1} bands were also sensibly sharpened, and slightly downshifted (Fig. 3). The typical band at 1747 cm^{-1} changed to a slight shoulder of a new sharp peak observed at 1716 cm^{-1}, accompanied by a deformed broad band at 1650 cm^{-1} (Fig. 3). The C=O stretching vibration at around 1710 cm^{-1} has been reported as characteristic of organic acids (cinnamics) which do not have a pronounced bipolar structure of the carbonyl group (Dimitrić-Marković et al., 2001). Additionally, a new peak was observed at 1517 cm^{-1} in films stored in the

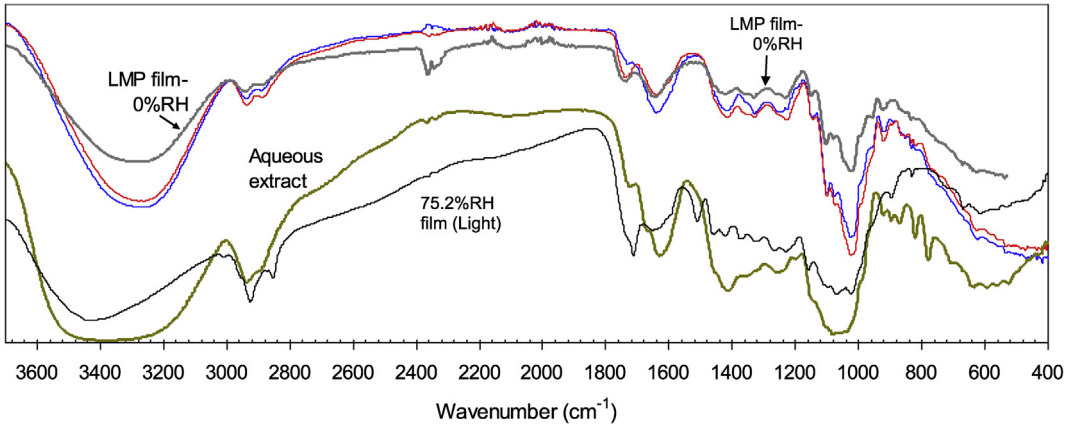

Fig. 3. FT-IR spectra of LMP-films equilibrated at 0% (grey line), 57.7% (red line) or 75.2%RH (blue line) in the dark, or at 75.2%RH in the light (black line), and of the freeze-dried cherry aqueous extract (green line). (For interpretation of the references to color in this figure legend, the reader is referred to the Web version of this article.)

light (Fig. 3), corresponding to the stretching vibration of an aromatic ring (C−C; C=C), which can be related to the catechol rings of quercetin and cyanidin derivatives, as well as of chlorogenic and neochlorogenic acids (Janković et al., 2009). This peak is also shown by feruloylated pectins of beet root cell walls (Synytsya et al., 2003). All these results can suggest that the mentioned phenolics interacted with the LMP polymer, constituent of the film matrix, through light accelerated reactions. According to Renard et al. (2015), pectins show high affinity in the interaction with polyphenols. The binding is due to a combination of hydrogen bonds and hydrophobic interactions, increasing the affinity with the degree of methyl-esterification of the homogalacturonans, and it is favored by increased ionic strength and decreased temperature.

The fingerprint zone (1200-950 cm^{-1}) that identified the polygalacturonic backbone of pectins for films stored in the dark (Pérez et al., 2009), was completely changed by the light influence, indicating that a new compound was formed (Fig. 3). Many bands between 1467 and 1236 cm^{-1} can be observed, as well as the broad band of noticeable lower intensity than that originally found between 1162 and 946 cm^{-1}. The original peak of pectins at 925 cm^{-1} disappeared, while a different peak at 906 cm^{-1} was observed. The shape of the broad band recorded between 1174 and 948 cm^{-1} from film stored under light was more similar to that recorded from the aqueous phenolic extract. In this latter case, the 1174-948 cm^{-1} band can be in part associated to anthocyanins. As studied by Ahn et al. (2017), pectin conjugated with rutin (cyanidin-3-*O*-rutinoside) produced a similar 1174-948 cm^{-1} band to that observed in LMP-films stored in the light, whereas pectin conjugated with quercetin originated a similar profile in the 1467-1236 cm^{-1} region.

The 1640 cm^{-1} broad band in the spectrum of films stored in the light can be also in part attributable to the −OH bending vibration of copigments of anthocyanins with other phenolics like hydroxycinnamic acids (Eiro and Heinonen, 2002) or cyanidin-quercetin copigment complex (Dimitrić-Marković et al., 2005), when compared to the spectrum recorded from the aqueous extract (Fig. 3).

The FTIR results can justify the heterogeneity observed through the different T_g values determined as amorphous regions of LMP films, involving interactions of the LMP macromolecules with glycerol, the water adsorbed, and the phenolic compounds.

3.5. Antioxidant capacity and stability of the phenolic compounds loaded in films

The antioxidant capacity of films was evaluated as the radical scavenging (DPPH assay) and ferric reducing (FRAP assay) abilities, expressed as L-(+)-ascorbic acid. Fig. 4a shows that both activities decreased significantly after 215 days of film storage with respect to the levels initially determined. Only the decay of DPPH activity increased significantly ($p < 0.05$) with the RH of equilibration. Light produced an additional decrease in the antioxidant capacity at 215 d.

The antioxidant capability of the edible films developed can be ascribed to the phenolics loaded in films. The concentration of each individual phenolic compound in the LMP film matrix at each storage time, $C_{Ph}(t)$ (eq. (2)), was determined during ≈220 days. The C_{Ph} decrease with the increase in time statistically fitted to a pseudo-first order ($z = 1$) kinetic (eq. (9)):

$$J = -\frac{1}{\nu}\frac{dn_{Ph}}{dt} = k'_{Ph} \cdot n^{Z}_{Ph} \quad (9)$$

because the natural logarithm of the experimentally determined $C_{Ph}(t)$ vs time gave a straight line at each storage condition studied (eq. (10)), which is the integrated form of the kinetic equation (eq. (9)):

$$\ln \frac{n_{Ph}(t)}{n_{Ph}(t=0)} = \ln C_{Ph}(t) = -\nu \cdot k'_{Ph} \cdot t \quad (10)$$

wherein J is the reaction rate at a constant temperature (25.0 °C) for a given phenolic compound, ν is the stoichiometric coefficient of the phenolic compound in its degradation reaction under air, at constant RH, n_{Ph} are the moles of a given phenolic compound at time t or initial time ($t = 0$), k_{Ph}' is the rate constant, z is the reaction order, $C_{Ph}(t)$ is the concentration of the phenolic compound at time t (eq. (2)). Considering $\nu = 1$, the slope obtained in eq. (10) gave directly the pseudo-first order rate constant (k_{Ph}') determined at 25.0 °C, whose values are reported in Table 4. The half-life time ($t_{1/2}$) for z = 1 was then calculated from each value of k_{Ph}' (eq. (11)), and also summarized in Table 4:

$$t_{1/2} = \frac{0.693}{\nu \cdot k'_{Ph}} \quad (11)$$

Anthocyanins were by far the least stable phenolics loaded in films at all storage conditions, whereas flavonols (dihydrokaempferol-glucoside and quercetin-3-*O*-rutinoside) were certainly the most stable components. According to Hernández-Herrero and Frutos (2015), anthocyanins' color can be stabilized by the presence of other phenolics through intermolecular copigmentation, and flavonols like quercetin-3-*O*-rutinoside (Table 4) are reported as the most efficient copigments. As anthocyanins can be directly responsible for the films' red color, their degradation is then expected to be also seen through the variation in the a^* and b^* color parameters. As seen in Table 5, a^* decreased with the increase in the storage time under darkness with a higher pseudo-zero order rate constant than b^*, which is coherent with the fastest anthocyanins-loss. Under light, a^* decreased but b^* increased with time according to a combined zero- and first-order-kinetic (De'Nobili et al., 2016), both reaching a plateau. Consequently, a persistent yellow-slightly reddish color is finally obtained at longer times, which can be ascribed to the remaining, most stable flavonols and also probably to the formation of color products.

The C_{Ph} decay for each phenolic compound in films was correlated with the variation of a^* and b^* with time, and the Spearman's correlation coefficients obtained are reported in Table 5. The highest correlation ($p < 0.0001$ and $p = 0.0001$) was observed between the positive a^* parameter and the anthocyanins at all storage conditions, suggesting that the decay in the red color of films was mainly due to the anthocyanins' degradation. Lower but highly significant correlation was also observed between the anthocyanin concentration decay and the decrease in the positive b^* (yellow component) values found in films stored in the dark or the increase in b^* (yellow component) values, under light. At all storage conditions, the film lightness (L^*) increased with the highest and significant correlation with the a* parameter decrease (Table 5). This can suggest that the film redness (a^*) due to the level of anthocyanins is which essentially contributed to the film darkness. Lower but significant correlations were also observed between L^* and b^*, which were inversely related for films stored in the dark, and positively related when stored under light (Table 5). The dihydrokaempferol-glucoside and quercetin-3-*O*-rutinoside were the only phenolics whose respective decaydid not correlate with the film color, except when the storage was performed under light, where the lowest but significant correlation coefficients were obtained (Table 5). The degradation of neochorogenic, chlorogenic and 3-*p*-coumaroylquinic acids correlated with the variation of a^* and b^* with notably lower significance than anthocyanins, and did it positively for films stored in the dark and negatively for films stored under light (Table 5).

On the other hand, the rate constants of decay of the neochlorogenic acid and anthocyanins at 25.0 °C constant were the only that depended on the RH of film storage, being directly related. Chlorogenic and 3-*p*-coumaroylquinic acids only differ in the cathechol group present in the first acid, which losses one −OH group to form the latter acid, whereas the neochlorogenic acid is the isomer of chlorogenic acid at the C1 of the *p*-coumaric acid rest. As indicated by Yamasaki et al. (1996), the flavylium cation of anthocyanin molecules is susceptible to the nucleophilic attack of water, with the subsequent formation of the colorless carbinol pseudobase or hemiketals. Water leads to the destruction of anthocyanin molecules, with spontaneous bleaching even in

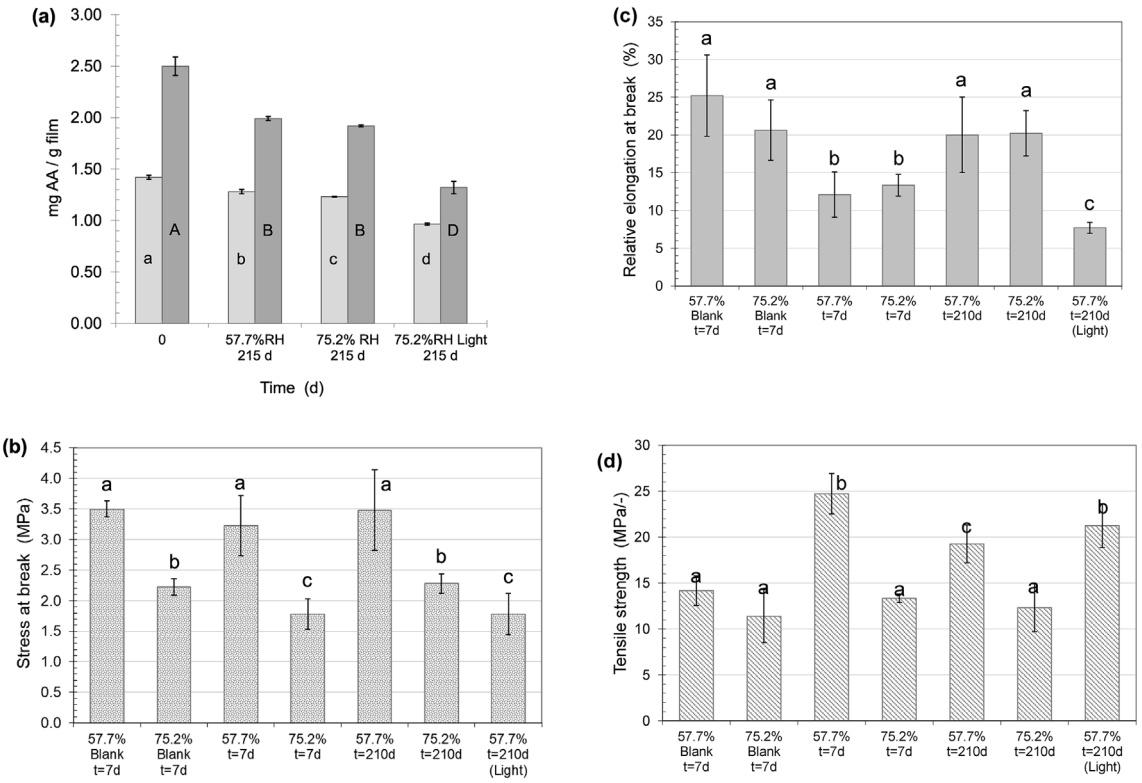

Fig. 4. Antioxidant capacity (**a**) determined through the DPPH (light grey bars) and FRAP (dark grey bars) assays, expressed as mg of L-(+)-ascorbic acid (AA) per g of film. Mechanical evaluation: stress (**b**), relative elongation or strain (**c**), and tensile strength (**d**) determined at film fracture (25 °C; 5 mm/min), from films equilibrated at the RH and stored for the time *t*. "Blank" are films made without phenolics. The same letters in a given assay or parameter mean non-significant ($p < 0.05$) differences.

Table 4
Pseudo-first-order rate constants of phenolic-decay kinetic (k_{Ph}')[a], and the calculated half-life time ($t_{1/2}$) for each phenolic compound in film, at 25.0 °C.

HR	Kinetic parameters[1]			
	Phenolic compounds (retention time; min)	$k_{Ph}' \times 10^3$ (d^{-1})	*p*	$t_{1/2}$ (months)
57.7% (dark)	**12.3**	4.3 ± 0.9[a]	< 0.0001	5.4
	16	3.0 ± 0.8[a]	0,002	7.7
	18	3.7 ± 0.6[a]	< 0.0001	6.2
	23	7.4 ± 0.6[b]	< 0.0001	3.1
	29	0.0278 ± 0.2[c]	**0,904**	829.4
	36	0.156 ± 0.3[c]	**0,613**	145.0
75.2% (dark)	**12.3**	7.2 ± 0.8[d]	< 0.0001	3.2
	16	1.8 ± 0.9[a]	0,0490	12.9
	18	5.3 ± 0.7[a]	< 0.0001	4.4
	23	12.0 ± 0.8[e]	< 0.0001	1.9
	29	0.303 ± 0.3[c]	**0,285**	76.3
	36	0.0318 ± 0.6[c]	**0,956**	726.4
75.2% (Light)	**12.3**	25 ± 2[f]	< 0.0001	0.9
	16	7.9 ± 1[g]	< 0.0001	2.9
	18	17 ± 1[h]	< 0.0001	1.4
	23	63 ± 6[i]	< 0.0001	0.36
	29	1.8 ± 0.2[j]	< 0.0001	12.6
	36	3.3 ± 0.4[k]	< 0.0001	7.0

[a] Mean and the standard deviation ($n = 3$) are reported. The same lower case letters in a column mean non significant differences ($p < 0.05$). Bold numbers in probability (*p*) mean that the slope (k_{Ph}') was not significantly different from zero.

neutral pH buffer, under aerobic conditions. Hence, for these compounds, the k_{Ph}' rate constant shown in equations (9) and (10) was actually the product of the bimolecular rate constant of reaction, which only depends on temperature, multiplied by the water concentration as nucleophile reactive. The decay of the DPPH activity in films (Fig. 4a) could be mainly related to that of the anthocyanins since both were RH dependent.

At 57.7% RH, there was non-significant difference between the rate constants of decay of the hydroxycynnamic acid derivatives, neither of the flavonols (Table 4). However, at 75.2% RH in the dark and light, the 3-*p*-coumaroylquinic acid was the most stable ($p < 0.0001$) of the hydroxycynnamic acids, while the neochlorogenic acid was the least stable ($p < 0.0001$) of them at all storage conditions. The light also increased considerably the degradation rate constants of the hydroxycinnamic acids (Table 4). Hence, the neochlorogenic and chlorogenic acids, which are constituted by a catechol ring conjugated with double bonds (α,β-unsaturated carbonyl substituent), were the hydroxycinnamic acid derivatives that degraded faster. UV light is harmful, though both visible light and near UV (300–400 nm) are important sources of reactive oxygen species, particularly singlet oxygen ($^1O_2$), the lowest excited electronic state of molecular oxygen (Goss-Sampson et al., 1995). Only by storage in the light, each flavonol compound showed decay rates significantly different from zero ($p < 0.0001$), being the quercetin-3-*O*-rutinoside the least stable of the flavonols (Table 4). Buchner et al. (2006) proposed that quercetin can be oxidized in air to a quinone structure, and solvent (water) molecules are then added in the C2-C3 double bond of the ring C. This double bond is absent in the dihydrokaempferol-glucoside compound loaded in films. Lightning was probably which triggered this oxidative reaction of quercetin in the equilibrated films. In spite of it, flavonols were significantly ($p < 0.0001$) more stable to lightning that the rest of the phenolics loaded in the LMP-films (Table 4). It was reported that

Table 5
Pseudo-zero (k_O) or combined zero and first order (k_O and k_1) kinetic rate constants[a] and initial color parameter in films. Spearman's correlation coefficients (r_S) obtained by comparison between the a^* or b^* color parameters and the concentration of each phenolic compound, or by comparison between the L^* and a^* or b^* color parameters, at the storage times.

HR	Kinetic equation parameters for film color					Spearman's correlation			
		$k_o \times 10^2$ (d^{-1})	$k_1 \times 10^2$	a^*, b^* or L^* (at $t = 0$)	r^2		Phenolic (retention time; min) or color parameter	r_S	p
57.7% (dark)	a^*	6.8 ± 0.4 [a]	—	—	0.964	a^*	**12.3**	0.7576	0.0149
							16	0.6848	0.0347
							18	0.8424	0.0037
							23	0.9758	< 0.0001
							29	0.1394	**0.7072**
							36	-0.1394	**0.7072**
	b^*	0.37 ± 0.02 [b]	—	—	0.975	b^*	**12.3**	0.7576	0.0149
							16	0.6848	0.0347
							18	0.8667	0.0022
							23	0.8788	0.0016
							29	0.0060	**1**
							36	-0.2606	**0.4697**
	L^*	3.4 ± 0.5 [c]	—	—	0.832	L^*	a^*	-0.9152	0.0005
							b^*	-0.8788	0.0016
75.2% (dark)	a^*	8.6 ± 0.4 [d]	—	—	0.981	a^*	**12.3**	0.9273	0.0003
							16	0.7333	0.0202
							18	0.8545	0.0029
							23	0.9515	0.0001
							29	0.2606	**0.4697**
							36	0.1152	**0.7589**
	b^*	0.47 ± 0.09 [b]	—	—	0.428	b^*	**12.3**	0.7576	0.0149
							16	0.7576	0.0149
							18	0.6364	0.0544
							23	0.7939	0.0088
							29	0.2727	**0.4483**
							36	0.1758	**0.6321**
	L^*	4.7 ± 0.5 [e]	—	—	0.894	L^*	a^*	-0.9515	0.0001
							b^*	-0.7939	0.0088
75.2% (Light)	a^*	10 ± 3 [f]	1.8 ± 0.1 [f]	52.5 ± 0.7	0.949	a^*	**12.3**	0.8303	0.0047
							16	0.9273	0.0003
							18	0.8909	0.0011
							23	0.9515	0.0001
							29	0.7818	0.0105
							36	0.7697	0.0126
	b^*	29 ± 4 [g]	1.0 ± 0.2 [g]	14.2 ± 0.2	0.943	b^*	**12.3**	-0.8061	0.0072
							16	-0.8545	0.0029
							18	-0.8667	0.0022
							23	-0.8788	0.0016
							29	-0.7091	0.0268
							36	-0.6970	0.0306
	L^*	52 ± 6 [h]	0.8 ± 0.1 [h]	31.6 ± 0.5	0.908	L^*	a^*	-0.9636	< 0.0001
							b^*	0.9152	0.0005

[a] Mean and the standard deviation ($n = 3$) are reported. The same lower case letters in a column mean non significant differences ($p < 0.05$).

flavonols scavenge singlet oxygen ($^1O_2$) formed in light, hence suffering photo-oxidation (Ávila et al., 2001). However, anthocyanins like cyanidin 3-*O*-glucoside and cyanidin 3-*O*-rutinoside also scavenge singlet oxygen through a charge-transfer mechanism, which is modulated by the total number of −OR substituents that increases the electron donating ability (De Rosso et al., 2008). Also, hydroxycinnamic acids exhibit singlet oxygen quenching through the electron-donating ability of the substituents, and the polarity of the solvent influences the quenching rate. Charge transfer is thereby attended to singlet oxygen quenching (Foley et al., 1999). Phenolic compounds having one hydroxyl group on their aromatic ring are less effective antioxidants than phenolics with the second hydroxyl group in the *ortho* or *para* position, but the presence of more than three hydroxyl groups on an aromatic ring does not improve the antioxidant activity. Because of this structural feature, 3-*p*-coumarylquinic acid is less active than neochlorogenic and chlorogenic acids as antioxidant and, hence in scavenging singlet oxygen, being then more stable during film storage under light (Table 4). Also, when films were stored in the dark. Among light-stored films, anthocyanins scavenged singlet oxygen more rapidly than the other phenolics, as inferred from their lowest stability, followed by the hydroxycinnamic acids (Table 4), suffering photo-bleaching.

Photosensitizer dyes (i.e. chlorophylls, porphyrins, bilirubin, quinone rings), which absorb radiation, are pro-oxidant molecules that can carry out the photo-oxidation reactions (Espinoza et al., 2016). It is proposed that anthocyanins, which were those that exhibited the fastest decay (Table 4), with red color vanishing as shown by the a^* parameter (Table 5), can absorb light through their higher amount of conjugated unsaturated (−C=C−C=O) bonds or π-electron configurations, acting as sensitizers for transformation of the triplet oxygen into the singlet oxygen. This is a bimolecular reaction between the light-activated (triplet state) flavinium cation of the cyanidins and the ground triplet oxygen molecule. Again, the k_{Ph}' rate constant in equation (10) is the product of the bimolecular rate constant of reaction, which only depends on temperature, multiplied by the triplet oxygen concentration. The singlet oxygen produced by the sensitizer can then be scavenged preferentially by the hydroxycinnamic acids and, in a lower extent, by

flavonols, but also by the anthocyanins (De Rosso et al., 2008). The scavenging of singlet oxygen is also a bimolecular mechanism and, hence, the k_{Ph}' rate constant (eq. (9)) included the true rate constant and the phenolic (scavenger) concentration.

By studying the role of the singlet oxygen in the photodegradation of plastics, Zweig and Henderson (1975) established that most classes of dye chromophores, including quinone and anthraquinone, were sensitizers in polymer films, absorbing light and transferring the absorbed energy to the atmospheric triplet ground oxygen, generating the metastable and reactive singlet oxygen, which can affect the polymers. As reported by Feild et al. (2001), since anthocyanins strongly absorb blue-green light, their accumulation in red autumn leaves may attenuate the quality and quantity of light captured by chlorophylls and carotenoids as leaves senesce.

In our work, the quercetin-3-*O*-rutinoside is that of the flavonols whose molecular structure adjusts to the requirements of the more favorable reaction with singlet oxygen (Morales et al., 2012). Coincidentally, it was the flavonol with the highest loss-rate constant in light-stored films (Table 4).

When evaluating the freeze-dried apple pomace and pulp powders as matrices for phytochemical retention, Lavelli and Kerr (2012) determined that the changes in the contents of flavonols, flavanols, dihydrochalcones, anthocyanins, and hydroxycinnamic acids during storage at a_W between 0.11 and 0.75, at 30 °C, were well-fitted by a first-order kinetic model. Simultaneously, the color parameters (L^*, a^*, b^*) changed according to a zero-order kinetic. In all cases, the kinetic-rates increased with the a_W. The cyanidin-3-*O*-galactoside was also the least stable of the phenolic compounds, with rate constants of 14×10^{-3} and $41 \times 10^{-3}\,d^{-1}$ at 0.56 and 0.75 a_W, respectively, whereas quercetin-3-*O*-galactoside was in general the most stable, with rate constants of 0.65×10^{-3} and $6.7 \times 10^{-3}\,d^{-1}$ at 0.56 and 0.75 a_W, respectively. Chlorogenic acid showed an intermediate stability, with rate constants of 0.97×10^{-3} and $2.2 \times 10^{-3}\,d^{-1}$ at 0.56 and 0.75 a_W, respectively.

Mrad et al. (2012) determined that the phenolic content decay into parallelepipedic pieces of pears was best fitted by a pseudo first-order reaction during convective drying, and the rate constants increased with the air temperature assayed, between 30 and 70 °C. As reported by Patras et al. (2010), the anthocyanins-degradation under isothermal heating followed a first order kinetic in juice and concentrate of sour cherry, strawberries and blackberries, as well as in other thermally processed food. The degradation reaction occurring at high temperatures involved deglycosylation followed by cleavage of the molecules.

A dry red powder from roselle calyces containing cyanidin-3-*O*-glucoside was produced by microencapsulation as a natural colorant and functional food ingredient by Idham et al. (2012), using maltodextrin, gum Arabic, combination of maltodextrin and gum Arabic, or soluble starch as matrices. The initial content of the anthocyanin in the microencapsulated powder was not reported, but the authors indicated that its decay studied at 4°, 25° and 37 °C was best fitted by the first-order kinetic model. The half-life times in the matrices varied between 3.4 months at 37 °C and 6.2 months at 4 °C when stored at the dehydrated state of the powder.

Sun et al. (2016) determined that the degradation trend of pelargonidin-3-*O*-glucoside in solution under an ultrasound treatment at 4 °C was consistent with a first-order reaction kinetic, increasing the rate constants from 1.69×10^{-2} to $6.72 \times 10^{-2}\,min^{-1}$ with the ultrasound power assayed (200–500 W range), and in parallel with the increase in the $^{\bullet}OH$ radical formation. The kinetic order of this radical mediated degradation of an anthocyanin also coincided with that observed for the anthocyanins and the other cherry phenolic compounds loaded in the LMP-films when stored under light, being actually pseudo-first order reactions of true bimolecular mechanisms, as above discussed.

3.6. Mechanical performance of films

After equilibration, the maximal normal stress (Fig. 4b) and relative deformation (strain) (Fig. 4c) at film failure were determined. Films made without phenolics, called "blank" films, permitted to observe that the presence of phenolics did not change significantly ($p < 0.05$) the stress at film fracture at the same RH of equilibration, except slightly at 75.2%RH (Fig. 4b). The increase in the RH of equilibration decreased significantly ($p < 0.05$) the fracture stress at all storage conditions. The stress diminished significantly ($p < 0.05$) for films stored under light at 75.2%RH (Fig. 4b). Simultaneously, the corresponding strain at break did not change significantly ($p < 0.05$) with the increase in the RH of film equilibration, but films stored under light (75.2%RH) showed the lowest strain (Fig. 4c). The latter result together with some lower corresponding stress of those recorded from films equilibrated at 75.2%RH (Fig. 4b), suggested that films stored under light were brittle. They showed low elongation, breaking then at some lower stress. The lowest value of strain and low stress at break led to the highest value of tensile strength (*TS*; eq. (6)) determined from films equilibrated for 210 days at 75.2%RH (Fig. 4d). Beyond a higher *TS*, the effect of light was to diminish the film deformability (Fig. 4c), which can suggest an increase of crosslinking in films. Just the presence of phenolics decreased significantly ($p < 0.05$) the film deformability at 7 days of film storage at both 57.7 and 75.2%RH, as compared to the corresponding "blank" films (Fig. 4c). This can demonstrate that an interaction between phenolics and the LMP-network occurred even in the dark. Under light, the film deformability suffered an additional decrease after 210 days of storage, contrary to that observed in films stored under darkness (Fig. 4c). The degradation of phenolics in the dark may lead to the final increase in the elongation of films at 210 days, reaching similar strain values to those of the "blank" films (Fig. 4c). The same is observed for *TS* (Fig. 4d). Far from plasticizing, the addition of phenolics antiplasticized the LMP network (Fig. 4c) and, hence, the light crosslinked the film matrix at longer storage period. FTIR results demonstrated the interaction between pectin and phenolics, which occurred mainly in films stored under light and, in a sensibly lower degree, in films stored at 75.2%RH in the dark (Fig. 3). The high interaction promoted by lightning was also explained by the lowest value of moisture content found (Table 3). Crosslinking in the polymeric network of films constrains the adsorption capacity of macromolecules and, hence, the moisture level reached at a given a_W or RH decreases.

For films containing phenolics, *TS* decreased when the RH of film equilibration increased (Fig. 4d), showing the plasticizing effect of the water adsorbed by the polymeric network.

4. Conclusions

Cherry phenolics extracted from the sugar exhausted *Prunus avium* homogenate by the 90°C-blanching water were best stabilized as red calcium crosslinked-LMP films (pH 3.46) under storage in the dark with lower RH (57.7%; 25 °C), because the anthocyanins-decay and, hence, the film red color intensity were RH dependent ($t_{1/2}$ = 3-2 months). On the contrary, flavonols (dihydrokaempferol-glucoside and quercetin-3-*O*-rutinoside) were stable at 57.7 and 75.2%RH ($t_{1/2}$ > 1.5 years). Light (75.2%RH) was highly detrimental for phenolics, and triggered LMP-matrix—phenolic interactions, which altered the film performance (decreased water content and deformability). In spite of the phenolics' degradation profiles, an 88% of antioxidant capacity, measured as radical scavenging activity, remained in films after 210 days of storage in the dark, and a 68% when stored under light, while a 78% of reducing activity remained in films at the end of the same period in the dark, and a 53% when stored under light. An antioxidant colored film matrix to stabilize phenolics, attractive for special purposes in food preservation, was then obtained.

Acknowledgements

For the financial support of the University of Buenos Aires [2014-2017 20020130100553BA], CONICET [2012-2014 PIP112-201101-00349], and ANPCyT [PICT 2012-1941; PICT 2013-2088; PICT 2015-2109]. We thank Lic. Graciela Guananja (CP-Kelco) for providing the pectin.

References

Ahn, S., Halake, K., Lee, J., 2017. Antioxidant and ion-induced gelation functions of pectins enabled bypolyphenol conjugation. Int. J. Biol. Macromol. 101, 776–782.
Ávila, V., Bertoletti, S.G., Criado, S., Pappano, N., Debattista, N., García, N.A., 2001. Antioxidant properties of natural flavonoids: quenching and generation of singlet molecular oxygen. Int. J. Food Sci. Technol. 36, 25–33.
Basanta, M.F., Marin, A., De Leo, S.A., Gerschenson, L.N., Erlejman, A.G., Tomás-Barberán, F.A., Rojas, A.M., 2016. Antioxidant Japanese plum (*Prunus salicina*) microparticles with potential for food preservation. J. Funct. Foods 24, 287–296.
Benbettaïeb, N., Assifaoui, A., Karbowiak, T., Debeaufort, F., Chambin, O., 2016. Controlled release of tyrosol and ferulic acid encapsulated in chitosan-gelatin films after electron beam irradiation. Radiat. Phys. Chem. 118, 81–86.
Borges, T.H., López, L.C., Pereira, J.A., Cabrera-Vique, C., Seiquer, I., 2017. Comparative analysis of minor bioactive constituents (CoQ10, tocopherols and phenolic compounds) in Arbequina extra virgin olive oils from Brazil and Spain. J. Food Compos. Anal. 63, 47–54.
Buchner, N., Krumbein, A., Rohn, S., Kroh, L.W., 2006. Effect of thermal processing on the flavonols rutin and quercetin. Rapid Commun. Mass Spectrom. 20, 3229–3235.
Chaovanalikit, A., Wrolstad, R.E., 2004. Anthocyanin and polyphenolic composition of fresh and processed cherries authors. J. Food Sci. 69 (1), FCT73–FCT83.
Cittadini, E.D., 2007. Sweet Cherries from the End of the World: Options and Constraints for Fruit Production Systems in South Patagonia. Wageningen University, Holland, Argentina Ph.D. thesis. http://edepot.wur.nl/41079, Accessed date: 26 July 2017.
Coutinho, I.B., Freitas, A., Maçanita, A.L., Lima, J.C., 2015. Effect of water content on the acid–base equilibrium of cyanidin-3-glucoside. Food Chem. 172, 476–480.
De Rosso, V.V., Moran Vieyra, F.E., Mercadante, A.Z., Borsarelli, C.D., 2008. Singlet oxygen quenching by anthocyanin's flavylium cations. Free Radic. Res. 42 (10), 885–891.
De'Nobili, M.D., Pérez, C.D., Navarro, D.A., Stortz, C.A., Rojas, A.M., 2013a. Hydrolytic stability of L-(+)-ascorbic acid in low methoxyl pectin films with potential antioxidant activity at food interfaces. Food Bioprocess Technol. 6, 186–197.
De'Nobili, M.D., Curto, L.M., Delfino, J.M., Soria, M., Fissore, E.N., Rojas, A.M., 2013b. Performance of alginate films for retention of L-(+)-ascorbic acid. Int. J. Pharm. 450, 95–103.
De'Nobili, M.D., Rojas, A.M., Abrami, M., Lapasin, R., Grassi, M., 2015. Structure characterisation by means of rheological and NMR experiments as a first necessary approach to study the L-(+)-ascorbic acid diffusion from pectin and pectin/alginate films to agar hydrogels that mimic food materials. J. Food Eng. 165, 82–92.
De'Nobili, M.D., Soria, M., Martinefski, M.R., Tripodi, V.P., Fissore, E.N., Rojas, A.M., 2016. Stability of L-(+)-ascorbic acid in alginate edible films loaded with citric acid for antioxidant food preservation. J. Food Eng. 175, 1–7.
Dimitrić-Marković, J.M., Mioć, U.B., Baranac, J.M., Nedić, Z.P., 2001. A study of the IR spectra of the copigments of malvin chloride with organic acids. J. Serb. Chem. Soc. 66 (7), 451–462.
Dimitrić-Marković, J.M., Baranac, J.M., Brnadić, T.P., 2005. Electronic and infrared vibrational analysis of cyanidin-quercetin copigment complex. Spectrochim. Acta 62, 673–680.
Eiro, M.J., Heinonen, M., 2002. Anthocyanin color behavior and stability during storage: effect of intermolecular copigmentation. J. Agric. Food Chem. 50, 7461–7466.
Espinoza, C., Trigos, A., Medina, M.E., 2016. Theoretical study on the photosensitizer mechanism of phenalenone in aqueous and lipid media. J. Phys. Chem. 120, 6103–6110.
Fasoli, M., Dell'Anna, R., Dal Santo, S., Balestrini, R., Sanson, A., Pezzotti, M., Monti, F., Zenoni, S., 2016. Pectins, hemicelluloses and celluloses show specific dynamics in the internal and external surfaces of grape berry skin during ripening. Plant Cell Physiol. 57 (6), 1332–1349.
Feild, T.S., Lee, D.W., Holbrook, N.M., 2001. Why leaves turn red in autumn. The role of anthocyanins in senescing leaves of red-osier dogwood. Plant Physiol. (Wash. D C) 127, 566–574.
Flores, S., Conte, A., Campos, C., Gerschenson, L., Del Nobile, M., 2007. Mass transport properties of tapioca-based active edible films. J. Food Eng. 81, 580–586.
Foley, S., Navaratnam, S., McGarvey, D.J., Land, E.J., Truscott, G., Rice-Evans, C.A., 1999. Singlet oxygen quenching and the redox properties of hydroxycinnamic acids. Free Radic. Biol. Med. 26 (9/10), 1202–1208.
Gómez-Mascaraque, L.G., Dhital, S., López Rubio, A., Gidley, M.J., 2017. Dietary polyphenols bind to potato cells and cellular components. J. Funct. Foods 37, 283–292.
Goss-Sampson, M., Vivian, A.J., Kelly, F.J., 1995. Free radicals, inflammation and eye diseases. In: Blake, D., Winyard, P.G. (Eds.), Immunopharmacology of Free Radical Species. Academic Press Ltd, London, pp. 127.
Hauke, J., Kossowski, T., 2011. Comparison of values of Pearson's and spearman's correlation coefficients on the same sets of data. Quaest. Geogr. 30 (2), 87–93.
Hernández-Herrero, J.A., Frutos, M.J., 2015. Influence of rutin and ascorbic acid in colour, plum anthocyanins and antioxidant capacity stability in model juices. Food Chem. 173, 495–500.
Huang, S., Ma, Y., Zhang, C., Cai, S., Pang, M., 2017. Bioaccessibility and antioxidant activity of phenolics in native and fermented Prinsepia utilis Royle seed during a simulated gastrointestinal digestion in vitro. J. Funct. Foods 37, 354–362.
Idham, Z., Muhamad, I.I., Sarmidi, M.R., 2012. Degradation kinetics and color stability of spray-dried encapsulated anthocyanins from *Hibiscus sabdariffa* L. J. Food Process. Eng. 35 (4), 522–542.
Idrovo Encalada, A.M., Basanta, M.F., Fissore, E.N., De'Nobili, M.D., Rojas, A.M., 2016. Carrot fiber (CF) composite films for antioxidant preservation: particle size effect. Carbohydr. Polym. 136, 1041–1051.
Janković, I.A., Šaponjić, Z.V., Čomor, M.I., Nedeljković, J.M., 2009. Surface modification of colloidal tio2 nanoparticles with bidentate benzene derivatives. J. Phys. Chem. C 113, 12645–12652.
Lavelli, V., Kerr, W., 2012. Apple pomace is a good matrix for phytochemical retention. J. Agric. Food Chem. 60, 5660–5666.
Liu, Y., Bandhari, B., Zhou, W., 2006. Glass transition and enthalpy relaxation of amorphous food saccharides: a Review. J. Agric. Food Chem. 54, 5701–5717.
Morales, J., Günther, G., Zanocco, A.L., Lemp, E., 2012. Singlet oxygen reactions with flavonoids. A theoretical-experimental study. PLoS One 7 (7), e40548.
Mrad, N.D., Boudhrioua, N., Kechaou, N., Courtois, F., Bonazzi, C., 2012. Influence of air drying temperature on kinetics, physicochemical properties, total phenolic content and ascorbic acid of pears. Food Bioprod. Process. 90 (3), 433–441.
Patras, A., Brunton, N.P., O'Donnell, C., Tiwari, B.K., 2010. Effect of thermal processing on anthocyanin stability in foods; mechanisms and kinetics of degradation. Trends Food Sci. Technol. 21, 3–11.
Pérez, C.D., Flores, S.K., Marangoni, A.G., Gerschenson, L.N., Rojas, A.M., 2009. Development of a high methoxyl-pectin edible film for retention of L-(+)-ascorbic acid. J. Agric. Food Chem. 57, 6844–6855.
Qadir, M.A., Shahzadi, S.K., Bashir, A., Munir, A., Shahzad, S., 2017. Evaluation of phenolic compounds and antioxidant and antimicrobial activities of some common herbs. Int. J. Anal. Chem 2017, 1–6. Article ID 3475738. https://doi.org/10.1155/2017/3475738.
Renard, C.M.G.C., Watrelot, A.A., Le Bourvellec, C., 2015. Interactions between polyphenols and polysaccharides: mechanisms and consequences in food processing and digestion. In: 29th EFFoST Int. Conf. Proceed. 10–12 November, Athens, Greece.
Sokal, R.R., Rohlf, J.B., 2000. Biometry: the Principles and Practice of Statistics in Biological Research, third ed. W. H. Freeman and Company, San Francisco (pp. 253–380).
Sun, J., Mei, Z., Tang, Y., Ding, L., Jiang, G., Zhang, C., Sun, A., Bai, W., 2016. Stability, antioxidant capacity and degradation kinetics of pelargonidin-3-glucoside exposed to ultrasound power at low temperature. Molecules 21, 1109. http://dx.doi.org/10.3390/molecules21091109.
Synytsya, A., Copikova, J., Jankovska, P., 2003. Spectroscopic estimation of feruloyl groups in sugar beet pulp and pectin. Int. Sugar J. 105, 481–488.
Taghvaei, M., Jafari, S.M., 2015. Application and stability of natural antioxidants in edible oils in order to substitute synthetic additives. J. Food Sci. Technol. 52 (3), 1272–1282.
Vankar, P.S., Shuklar, D., 2011. Natural Dyeing with anthocyanins from Hibiscus rosa sinensis flowers. J. Appl. Polym. Sci. 122 (5), 3361–3368.
Xiao, H.W., Pan, Z., Deng, L.Z., El-Mashad, H.M., Yang, X.H., Mujumdar, A.S., Gao, Z.J., Zhang, Q., 2017. Recent developments and trends in thermal blanching-A comprehensive review. Inf. Proc. Agric 4, 101–127.
Yamasaki, H., Uefuji, H., Sakihama, Y., 1996. Bleaching of the red anthocyanin induced by superoxide radical. Arch. Biochem. Biophys. 332, 183–186.
Zweig, A., Henderson Jr., W.A., 1975. Singlet oxygen and polymer photooxidations. I. Sensitizers, quenchers, and reactants. J. Polym. Sci. 13, 717–736.